Cooperative Multi-AUV Localization Using Distributed Extended Information Filter

Gao Rui and Mandar Chitre
ARL, Tropical Marine Science Institute, National University of Singapore

***Abstract*—Cooperative multi-AUV localization has the potential to outperform single-AUV localization, by taking advantage of data sharing among the team members. Unlike terrestrial communication links, underwater communication links have many issues pertaining to the channel stability and bandwidth, and therefore a decentralized localization is preferred. However this opens up new challenges to team members working in cooperation. This paper uses analytical examples to illustrate the cooperation problems in the decentralized architecture. To solve these problems, we propose a new cooperative multi-AUV localization algorithm using distributed extended information filter (DEIF). The proposed method only requires small transmission packets and is designed for use under constrained underwater communication. It is robust to packet loss, providing consistent position estimates when fusing correlated data. We demonstrate the effectiveness and advantages of the proposed method with comparative results using data from simulation and field experiments.**

I. Introduction

Autonomous underwater vehicles (AUVs) traditionally localize themselves using the vehicle's own sensor data, such as GPS (when available), compass, altimeter, etc. In applications where multiple vehicles operate in an area simultaneously, cooperative multi-vehicle localization utilizes sensor data shared across the team and has the potential to outperform single-vehicle localization. Underwater communication links typically suffer from low bandwidth, high latency and significant packet loss, as compared to terrestrial communication links. It is therefore impractical for a team of AUVs to collate all sensor data centrally, and consquently a decentralized estimation algorithm is preferred.

There are two key challenges in decentralized cooperative multi-AUV localization. The first challenge arises from limited bandwidth. Due to this limitation, traditional methods send up-to-date estimates, instead of the raw measurements in the history. This causes information loss in cooperative localization. An empirical study [1] shows that the available bandwidth in underwater communication severely limits cooperative localization performance. The second challenge pertains to tracking of the inter-vehicle correlation. As data are exchanged between AUVs, the state estimates of the AUVs become correlated. Underestimation of the inter-vehicle correlation leads to estimation overconfidence. This overconfidence prevents utilization of subsequent useful information. Existing methods typically yield pessimistic estimates by either avoiding the fusion of correlated data [2], or assuming maximum correlation in the whole state [3]–[5] or separated states [6].

In this paper, we use extended information filter (EIF) - an inverse covariance form of the Kalman filter [7]. The reason is that the local prediction and measurement information can be encapsulated into a single message and acoustically transmitted in a small-sized packet. The decentralized EIF was first implemented in a single-beacon cooperative localization in [8]. We describe the detailed design and implementation of a distributed EIF (DEIF) localization for a team of cooperative AUVs, where no single AUV functions as a beacon possessing accurate position information. The proposed method is designed to record the correlation from the most recent cooperation, providing consistent position estimates even when there is packet loss.

This paper is organized in the following way: Section II gives analytical examples to illustrate the problems of underwater communication using distributed estimation. Section III formulates the cooperative localization problem and Section IV reports the detailed design and implementation of the DEIF method. In Section V, we demonstrate the effectiveness and advantages of the proposed method with comparative results using both simulated and experimental data.

II. Illustrative Examples

In this section, we use some simple examples to illustrate the problems with traditional approaches and show how our proposed DEIF overcomes these problems.

A. Limited Bandwidth

Let us start with a 2-step example: with known prior knowledge about their states x_1 and x_2, two vehicles : (1) take local measurements z_1 and z_2 about their states, and (2) communicate their states along with a relative distance measurement z_r. We assume the initial correlation between vehicles is known. Fig. 1(a) shows the centralized and decentralized estimation architectures. The centralized architecture collates the states (or measurements) by stacking them together; it updates the stacked states with the stacked measurements. The decentralized architecture follows the two steps: vehicle updates its state with the local measurement to obtain a local updated state estimate (x_1' or x_2'), and after communication, a relative measurement is used to update the stacked state estimates. Kalman filter [9] is used in both architectures. We also implement the EIF [7] in the decentralized architecture. The estimation results are shown in Fig. 1(b). We can see that by transmitting only up-to-date estimates, the decentralized

978-1-5090-2442-1/16/$31.00 ©2016 IEEE

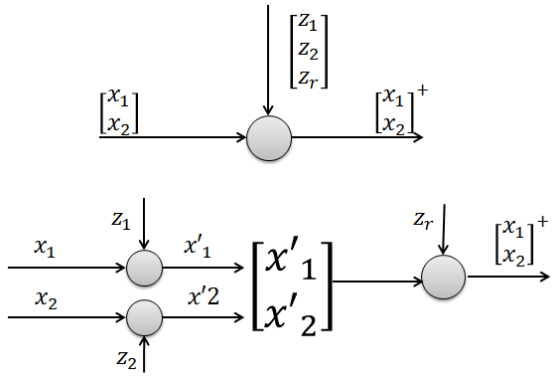

(a) Centralized (upper) vs. decentralized (lower) architectures: The grey circle indicates a measurement update.

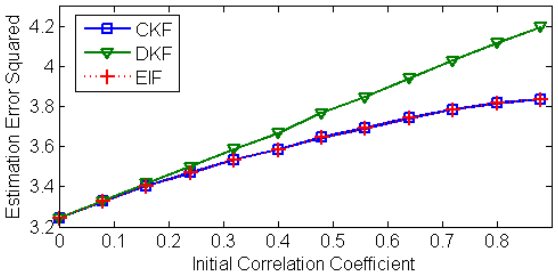

(b) Estimation performance: EIF overlaps with CKF.

Fig. 1. A 2-step example with CKF, DKF and EIF.

Kalman filter (DKF) produces larger errors than the centralized Kalman filter (CKF). This can be explained in the context of information theory: the mutual information between the states is reduced by conditioning on local measurements. There is information loss from fusing the processed data, instead of raw data.

To maintain the same performance as the centralized estimation, DKF requires a full storage and transmission of the historical information. If there are n steps of local propagation and measurements before the cooperation, the packet size for transmission will increase as $\mathcal{O}(n)$. In the other hand, EIF is able to avoid the information loss that DKF suffers, and performs as well as the CKF using transmissions of fixed, small-sized packets.

B. Inter-vehicle Correlation

We demonstrate the danger of overconfidence in a 3-AUV cooperative localization, where AUVs broadcast their state estimates in a round-robin fashion. The estimation error of AUV 1 is shown in Fig. 2. At 10 seconds, all AUVs submerge and lose GPS position measurements, but continue to communicate with each other. At 110 seconds, AUV 2 obtains a high-quality position measurement (say, by surfacing and obtaining a GPS fix). AUV 1's localization is improved by fusing estimates from AUV 2.

A naïve Kalman filter (NKF) simply ignores the correlation among vehicles; it assumes an improvement in estimate by

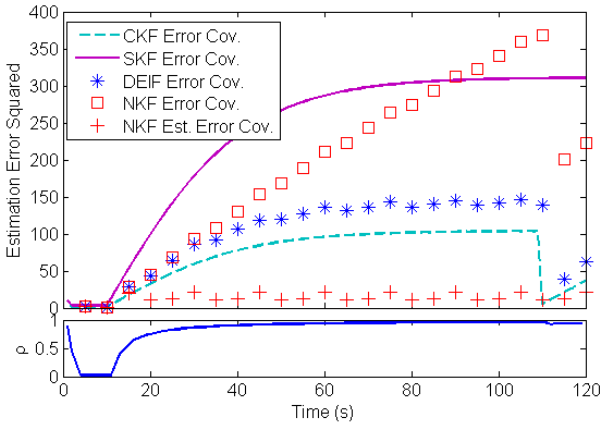

Fig. 2. Performance of AUV 1 in a 3-AUV cooperative localization example: ρ is the correlation coefficient between AUV 1 with other AUVs.

fusing data from 'independent' sources, while in fact there is no improvement from double counting the shared information. The estimated error covariance of NKF appears to be very low, but the actual estimation error diverges quickly. Its performance can be even worse than single vehicle localization (SKF). When a high quality measurement is obtained by AUV 2 at 110 seconds, the useful information provided by AUV 2 is not fully utilized at AUV 1; the improvement on AUV 1's localization is much smaller than it should be.

Our proposed method using DEIF (introduced in Section IV) performs well, and produces results that are quite close to the ideal (but infeasible) CKF.

III. Problem Formulation

At a discrete time step k, let the position state of a vehicle be x_k. For example, x is a state vector containing the easting/northing locations. From time step k to $k+1$ the vehicle propagates in a way such that

$$x_{k+1} = f(x_k, \mu_k) + \omega_k \tag{1}$$

where $f(\cdot)$ is the process function with Jacobian matrix $\mathbf{F}_k$, μ_k is the control input, and ω_k is the zero-mean Gaussian process noise with covariance matrix $\mathbf{Q}_k$.

A local observation can be made directly or indirectly about vehicle's position. An example of a direct observation would be the acquisition of a GPS fix. An indirect observation can be the altitude measurement based on a bathymetry map. Another example is the measurement indicating vehicle's relative location with respect to a fixed beacon or boat. Generally, the local observation is modeled as

$$z_k = h(x_k) + \nu_k \tag{2}$$

where the measurement error ν_k is zero-mean Gaussian with covariance $\mathbf{R}_k$. The observation function $h(\cdot)$ has a Jacobian matrix $\mathbf{H}_k$.

In the multi-vehicle cooperation, a vehicle encodes its information into acoustic packets and broadcasts as a Peer

Vehicle (PV). Other vehicles in the team receive the packets as Receiving Vehicles (RVs). If the team is synchronized, the one-way travel time of the acoustic signals is simply the difference between the time-of-launch and time-of-arrival. The distance from the PV to an RV is obtained, given the propagation speed of underwater signals. The observation model is

$$r_k = ||x_{k,\mathrm{R}} - x_{k,\mathrm{P}}|| + \upsilon_k \tag{3}$$

where the operator $||\cdot||$ denotes the Euclidean norm, and υ_k is the zero-mean Gaussian noise with covariance $\mathbf{V}_k$. To minimize the effect of nonlinearity, we assume the vehicles are far away from each other so that after the relative measurement update, the error in position estimation can be modeled as a 2-dimensional zero-mean Gaussian random variable.

We assume noise is independent of each other.

IV. Distributed Extended Information Filter and Implementation

Assuming the position state vector x is Gaussian distributed, the associated information matrix and information vector in an EIF is

$$\begin{aligned} \Lambda &= \Sigma^{-1} \\ \eta &= \Lambda u \end{aligned} \tag{4}$$

where u is the expected value and Σ is the covariance, i.e.,

$$\begin{aligned} u &= \mathbb{E}(x) \\ \Sigma &= \mathbb{E}[(x-u)(x-u)^\top] \end{aligned} \tag{5}$$

At time step k, each vehicle keeps an information set $(\mathbf{x}_k, \mathbf{\Sigma}_k, \Lambda_p, \eta_p)$. $\mathbf{x}_k$ is the combined 3-state vector $\mathbf{x}_k = [x_k^\top, x_t^\top, x_c^\top]^\top$ with the corresponding covariance matrix $\mathbf{\Sigma}_k$. x_k is the current position state. t denotes the time step when the most recent cooperation is made. During this cooperation, if a broadcast from a PV with position state x_c is received, this vehicle's position is updated as x_t. If this vehicle broadcasts at time step t as a PV, x_c is dummy and x_t is considered fully correlated with the team. We denote $\mathbf{x}_p = [x_t^\top, x_c^\top]^\top$ and therefore $\mathbf{x}_k = [x_k^\top, \mathbf{x}_p^\top]^\top$. (Λ_p, η_p) is the information pair (information matrix and vector) corresponding to $\mathbf{x}_p$.

A. Initialization

At time step $k = 0$, the initial position x_0 is assigned to x_t. We assume that all vehicles are deployed independently, i.e., the initial position has no correlation with the team and x_c is assigned a dummy value.

B. Local prediction

Let (Λ_k, η_k) be the information pair for $\mathbf{x}_k = [x_k^\top, \mathbf{x}_p^\top]^\top$, and x_{k+1} be the predicted state from x_k according to the process model. We augment the state vector with the predicted state and we have $\tilde{\mathbf{x}}_{k+1} = [x_{k+1}^\top, x_k^\top, \mathbf{x}_p^\top]^\top$. According to [7], the augmented state vector has an associated information pair given by

$$\tilde{\Lambda}_{k+1} = \begin{bmatrix} \mathbf{Q}_k^{-1} & -\mathbf{Q}_k^{-1}\mathbf{F}_k & \mathbf{0} \\ -\mathbf{F}_k^\top\mathbf{Q}_k^{-1} & \mathbf{F}_k^\top\mathbf{Q}_k^{-1}\mathbf{F}_k & \mathbf{0} \\ \mathbf{0} & \mathbf{0} & \mathbf{0} \end{bmatrix} + \begin{bmatrix} \mathbf{0} & \mathbf{0} & \mathbf{0} \\ \mathbf{0} & & \\ \mathbf{0} & & \Lambda_k \end{bmatrix}$$

$$\tilde{\eta}_{k+1} = \begin{bmatrix} \mathbf{Q}_k^{-1}(f(u_k,\mu_k) - \mathbf{F}_k u_k) \\ -\mathbf{F}_k^\top\mathbf{Q}_k^{-1}(f(u_k,\mu_k) - \mathbf{F}_k u_k) \\ \mathbf{0} \end{bmatrix} + \begin{bmatrix} \mathbf{0} \\ \eta_k \end{bmatrix}$$

We can see that in an EIF, the prediction information is contained in the first term of the addition, with zeros padded accordingly. Meanwhile, we only see non-zero entries in the off-diagonal blocks between states at consecutive time steps. This agrees with the Markov process assumption stating that prediction for the future state solely depends on the most recent state.

The local prediction is implemented in the Kalman filter form. The 3-state vector $\mathbf{x}_{k+1} = [x_{k+1}^\top, x_t^\top, x_c^\top]^\top$ is obtained with the predicted state x_{k+1}

$$x_{k+1} = f(x_k, \mu_k) \tag{6}$$

The associated covariance $\mathbf{\Sigma}_{k+1}$ is predicted as

$$\mathbf{\Sigma}_{k+1} = \begin{bmatrix} \mathbf{F}_k & \mathbf{0} & \mathbf{0} \\ \mathbf{0} & \mathbf{I} & \mathbf{0} \\ \mathbf{0} & \mathbf{0} & \mathbf{I} \end{bmatrix} \mathbf{\Sigma}_k \begin{bmatrix} \mathbf{F}_k & \mathbf{0} & \mathbf{0} \\ \mathbf{0} & \mathbf{I} & \mathbf{0} \\ \mathbf{0} & \mathbf{0} & \mathbf{I} \end{bmatrix}^\top + \begin{bmatrix} \mathbf{Q}_k & \mathbf{0} & \mathbf{0} \\ \mathbf{0} & \mathbf{0} & \mathbf{0} \\ \mathbf{0} & \mathbf{0} & \mathbf{0} \end{bmatrix} \tag{7}$$

We now have the information set $(\mathbf{x}_{k+1}, \mathbf{\Sigma}_{k+1}, \Lambda_p, \eta_p)$.

C. Local measurement update

The measurement matrix $\mathbf{H}_k$ is sparse as it only affects a few subblocks within the corresponding entry for x_k in the information pair. It allows an additive update to the information matrix and vecotr [7]

$$\begin{aligned} \Lambda_k^+ &= \Lambda_k + \mathbf{H}_k^\top\mathbf{R}_k^{-1}\mathbf{H}_k \\ \eta_k^+ &= \eta_k + \mathbf{H}_k^\top\mathbf{R}_k^{-1}(z_k - h(u_k) - \mathbf{H}_k u_k) \end{aligned} \tag{8}$$

where the superscript $+$ means the observation is made up to and including time step k. Note that the local measurement may not be available at every time step.

We implement the local measurement update in a standard Kalman filter form, and obtain the information set $(\mathbf{x}_{k+1}^+, \mathbf{\Sigma}_{k+1}^+, \Lambda_p, \eta_p)$.

D. Cooperative localization with relative measurement

We denote the information set kept at the PV as $(\mathbf{x}_k, \mathbf{\Sigma}_k, \Lambda_p, \eta_p)_\mathrm{P}$. Similarly, the subscript for the information set is R for the RV. It should be noted that in a team containing more than two vehicles, the time step t recorded at PV and RV may not be the same.

1) Delta information for cooperation: The delta information [8] is defined as the difference in information matrix and vector, from the most recent cooperation to the current time step.

With the information pair (Λ_k, η_k) obtained from Equation (4), both the PV and RV form their delta information

$$\bar{\Lambda}_k = \begin{bmatrix} \Delta\Lambda_{k,\mathrm{R}} & \cdots & \mathbf{0} \\ \vdots & \ddots & \vdots \\ \mathbf{0} & \cdots & \mathbf{0} \end{bmatrix} + \begin{bmatrix} \mathbf{0} & \cdots & \mathbf{0} & \cdots & \mathbf{0} \\ \vdots & \vdots & \vdots & \vdots & \vdots \\ \mathbf{0} & \cdots & \bar{\Lambda}_t & \cdots & \mathbf{0} \\ \vdots & \vdots & \vdots & \vdots & \vdots \\ \mathbf{0} & \cdots & \mathbf{0} & \cdots & \mathbf{0} \end{bmatrix} + \begin{bmatrix} \mathbf{0} & \cdots & \mathbf{0} \\ \vdots & \ddots & \vdots \\ \mathbf{0} & \cdots & \Delta\Lambda^*_{k,\mathrm{P}} \end{bmatrix}$$
$$\bar{\eta}_k = \begin{bmatrix} \Delta\eta_{k,\mathrm{R}} \\ \vdots \\ \mathbf{0} \end{bmatrix} + \begin{bmatrix} \mathbf{0} \\ \vdots \\ \bar{\eta}_t \\ \vdots \\ \mathbf{0} \end{bmatrix} + \begin{bmatrix} \mathbf{0} \\ \vdots \\ \Delta\eta^*_{k,\mathrm{P}} \end{bmatrix} \tag{12}$$

$(\Delta\Lambda_k, \Delta\eta_k)$ such that

$$\begin{aligned} \Delta\Lambda_k &= \Lambda_k - \begin{bmatrix} \mathbf{0} & \mathbf{0} \\ \mathbf{0} & \Lambda_p \end{bmatrix} \\ \Delta\eta_k &= \eta_k - \begin{bmatrix} \mathbf{0} \\ \eta_p \end{bmatrix} \end{aligned} \tag{9}$$

The PV broadcasts the delta information $(\Delta\Lambda_k, \Delta\eta_k)_\mathrm{P}$ together with $(\mathbf{x}_k, \mathbf{\Sigma}_k)_\mathrm{P}$ in a packet. The RV receives the packet and obtains the acoustic ranging as well.

2) Incorporating the delta information: When the broadcast from PV is received, the RV firstly forms the information matrix and information vector corresponding to the combined state vector $[x_{k,\mathrm{R}}^\top, x_{t,\mathrm{R}}^\top, x_{t,\mathrm{P}}^\top, x_{k,\mathrm{P}}^\top]^\top$. The information matrix consists of three parts: the delta information from the PV $\Delta\Lambda_{k,\mathrm{R}}$, the delta information from the RV $\Delta\Lambda_{k,\mathrm{P}}$, and the information matrix $\bar{\Lambda}_t$ corresponding to $[x_{t,\mathrm{R}}^\top, x_{t,\mathrm{P}}^\top]^\top$.

Assuming the states $x_{c,\mathrm{R}}$ and $x_{c,\mathrm{P}}$ are from the same source and fully correlated, a bounding joint covariance for states $x_{t,\mathrm{R}}$ and $x_{t,\mathrm{P}}$ can be derived. At both PV and RV sides, given the covariance matrix $\Sigma_p = \begin{bmatrix} \Sigma_t & \Sigma_{tc} \\ \Sigma_{ct} & \Sigma_c \end{bmatrix}$ (corresponding to $\mathbf{x}_p = [x_t^\top, x_c^\top]^\top$), the split form for x_t is

$$\begin{aligned} \Sigma_t &= \Sigma_{\text{IND.}} + \Sigma_{\text{DEP.}} \\ \Sigma_{\text{IND.}} &= \Sigma_t - \Sigma_{tc}\Sigma_c^{-1}\Sigma_{ct} \\ \Sigma_{\text{DEP.}} &= \Sigma_{tc}\Sigma_c^{-1}\Sigma_{ct} \end{aligned} \tag{10}$$

The reason is that $x_t - \Sigma_{tc}\Sigma_c^{-1}x_c$ and x_c are independent, and x_c represents the source of information shared from the team.

The bounding joint covariance matrix for $[x_{t,\mathrm{R}}^\top, x_{t,\mathrm{P}}^\top]^\top$ is therefore $\begin{bmatrix} \Sigma_{\text{IND.,R}} + \frac{\Sigma_{\text{DEP,R}}}{\kappa} & \mathbf{0} \\ \mathbf{0} & \Sigma_{\text{IND.,P}} + \frac{\Sigma_{\text{DEP,P}}}{1-\kappa} \end{bmatrix}_t$, $\kappa \in [0, 1]$. The value of κ is obtained by minimizing the error covariance of RV after the relative measurement update. The corresponding information pair for $[x_{t,\mathrm{R}}^\top, x_{t,\mathrm{P}}^\top]^\top$ is formed as

$$\begin{aligned} \bar{\Lambda}_t &= \begin{bmatrix} \Sigma_{\text{IND.,R}} + \frac{\Sigma_{\text{DEP,R}}}{\kappa} & \mathbf{0} \\ \mathbf{0} & \Sigma_{\text{IND.,P}} + \frac{\Sigma_{\text{DEP,P}}}{1-\kappa} \end{bmatrix}_t^{-1} \\ \bar{\eta}_t &= \bar{\Lambda}_t \bar{u}_t \end{aligned} \tag{11}$$

where $\bar{u}_t = \mathbb{E}([x_{t,\mathrm{R}}^\top, x_{t,\mathrm{P}}^\top]^\top)$.

The information pair corresponding to the combined state vector $[x_{k,\mathrm{R}}^\top, x_{t,\mathrm{R}}^\top, x_{t,\mathrm{P}}^\top, x_{k,\mathrm{P}}^\top]^\top$ is formed in Equation (12), where $\Delta\eta^*_{k,\mathrm{P}}$ and $\Delta\Lambda^*_{k,\mathrm{P}}$ are the rearranged $\Delta\eta_{k,\mathrm{P}}$ and $\Delta\Lambda_{k,\mathrm{P}}$, according to the reversed sequence $[x_{t,\mathrm{P}}^\top, x_{k,\mathrm{P}}^\top]^\top$. Zeros are padded before and after, where needed. The zero padding and addition are illustrated in Fig. 3.

3) Relative measurement update: With the information pair $(\bar{\Lambda}_k, \bar{\eta}_k)$, a measurement update can be made in the same way as Equation (8), with z_k replaced by r_k, and $\mathbf{R}_k$ replaced by $\mathbf{V}_k$. The Jacobian matrix $\mathbf{H}_k$ is calculated based on the observation model in Equation (3).

4) Information set update: After broadcasting out its information set, PV considers its state x_k as fully correlated with the team, and assigns it to x_t. States and their covariances at time steps prior to k are discarded. The RV assigns the updated $x_{k,\mathrm{R}}$ to x_t. The received $x_{k,\mathrm{P}}$ is recorded as x_c. At both sides, the most recent cooperation time t is assigned the value of k. The corresponding information pair (Λ_p, η_p) is recorded.

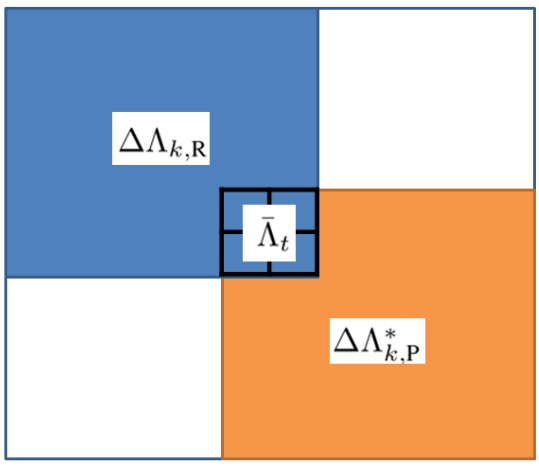

Fig. 3. Illustration of incorporating delta information in simple addition.

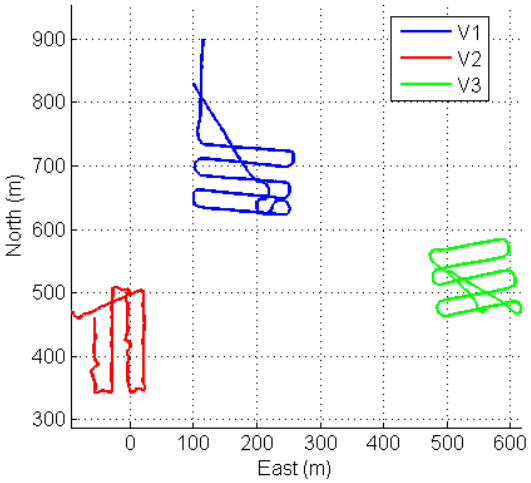

Fig. 4. Cooperative localization results with field data.

V. Simulation Studies using Field Experiment Data

We compare the performance of the proposed DEIF with several other methods using both simulated data and experimental data. The experimental data was collected from a team of three vehicles executing lawnmower surveys in Singapore waters (Fig. 4). While executing the planned path, vehicles experience propagation noise caused by choppy water, system hardware, etc. Local measurements such as GPS positions (if the vehicle is on the surface), or bathymetric measurements (for submerged vehicles in a known terrain), are fused to improve localization. Vehicles do not get good local measurements about their positions all the time. For example, GPS signals do not penetrate water when vehicles submerge throughout the mission; the positioning performance offered by bathymetric measurements strongly depend on the significance of the topography variations [10]. The cooperation happens when one vehicle broadcasts its information set and the other two vehicles receive.

A. Simulated data

The simulated data is designed to agree with the experimental data in Section V-B, using identical sensor characteristics and the same trajectories. In this simulation, vehicles take turns to broadcast their information every 10 seconds. The transmission packets are lost at a rate of p_l. In the first 100 seconds, all vehicles cruise on surface and have GPS fixes. Only Vehicle 2 re-surfaces at 420 seconds for 50 seconds.

The results are evaluated using two metrics: the normalized estimation error squared (NEES) and root mean square error (RMSE). The NEES provides a measurement of estimation consistency and is defined as [11]

$$\epsilon_k = \frac{1}{N}\sum_{i=1}^{N}(\hat{x}_k^{(i)} - x_k^{(i)})^\top (\Sigma_k^{(i)})^{-1}(\hat{x}_k^{(i)} - x_k^{(i)}) \tag{13}$$

where at each time step k, $\hat{x}$ is the estimate of the state x, with estimated error covariance Σ. Therefore $(\hat{x} - x)$ is the actual estimation error given, and Σ is the error covariance estimated by the vehicle. The superscript (i) denotes the result from the run i and there is in total N runs. Under ideal conditions, the NEES has an n_x (dimension of the state x, in our case $n_x = 2$) degree-of-freedom chi-square distribution. The RMSE records the estimated error in distance and is defined as

$$\xi_k = \sqrt{\frac{1}{N}\sum_{i=1}^{N}||\hat{x}_k^{(i)} - x_k^{(i)}||^2} \tag{14}$$

Fig. 5 shows the NEES and RMSE over 10 runs for Vehicle 3 at different packet loss rate. The arrows indicate an example of successful reception of the packets. At all packet loss rates, NKF claims to have the lowest RMSE among all the filters but has severe problem on estimation consistency. Especially when vehicles communicate at high frequency (Fig. 5(a)), the estimation errors given by NKF are in fact much larger than the errors it believes to be (shown as large NEES values). When vehicles communicate infrequently and are mostly independent of each other (Fig. 5(d)), the näive assumption by NKF is almost met, and therefore a consistent estimation is given.

We also compare the proposed method with SCI filter. In the SCI filter, let the estimated error covariance for PV and RV be $\mathbf{P}_{\text{PV}}$ and $\mathbf{P}_{\text{RV}}$. Therefore in Equation (13) and (14), the NEES and RMSE for SCI filter are calculated with $\mathbf{P}$ instead of Σ. According to [12], each state consists of correlated component and independent component, whose covariances are in summation form as

$$\begin{aligned}\mathbf{P}_{\text{PV}} &= \mathbf{P}_{\text{DEP.,P}} + \mathbf{P}_{\text{IND.,P}} \\ \mathbf{P}_{\text{RV}} &= \mathbf{P}_{\text{DEP.,R}} + \mathbf{P}_{\text{IND.,R}}\end{aligned} \tag{15}$$

We omit the superscript time step k for simplicity. As the range-only measurement is not enough to formulate a full estimate of the RV position, SCI filter in [12] can not be applied directly for the cooperation. We follow the idea of SCI and form a bounding joint covariance $\bar{\mathbf{P}}$ for the combined state vector $[x_{\text{RV}}^\top, x_{\text{PV}}^\top]^\top$. We have

$$\begin{aligned}\bar{\mathbf{P}} &= \begin{bmatrix} \mathbf{P}_{\text{IND.,R}} + \frac{\mathbf{P}_{\text{DEP.,R}}}{\kappa} & \mathbf{0} \\ \mathbf{0} & \mathbf{P}_{\text{IND.,P}} + \frac{\mathbf{P}_{\text{DEP.,P}}}{1-\kappa} \end{bmatrix} \\ &= \begin{bmatrix} \mathbf{P}_{\text{IND.,R}} & \mathbf{0} \\ \mathbf{0} & \mathbf{P}_{\text{IND.,P}} \end{bmatrix} + \begin{bmatrix} \frac{\mathbf{P}_{\text{DEP.,R}}}{\kappa} & \mathbf{0} \\ \mathbf{0} & \frac{\mathbf{P}_{\text{DEP.,P}}}{1-\kappa} \end{bmatrix} \\ &= \bar{\mathbf{P}}_{\text{IND.}} + \bar{\mathbf{P}}_{\text{DEP.}}\end{aligned} \tag{16}$$

The range measurement is used to update the combined state vector in standard Kalman filter method. The value of $\kappa \in [0, 1]$ is determined by minimizing the updated error covariance of the RV. The independent component for RV is obtained in the corresponding entries of the combined independent component

$$\bar{\mathbf{P}}_{\text{IND.}}^{+} = (\mathbf{I} - \mathbf{K})\bar{\mathbf{P}}_{\text{IND.}}(\mathbf{I} - \mathbf{K})^\top + \mathbf{K}\mathbf{V}\mathbf{K}^\top \tag{17}$$

where $\mathbf{K}$ is the Kalman gain obtained from range measurement, $\mathbf{I}$ is the identity matrix of corresponding size.

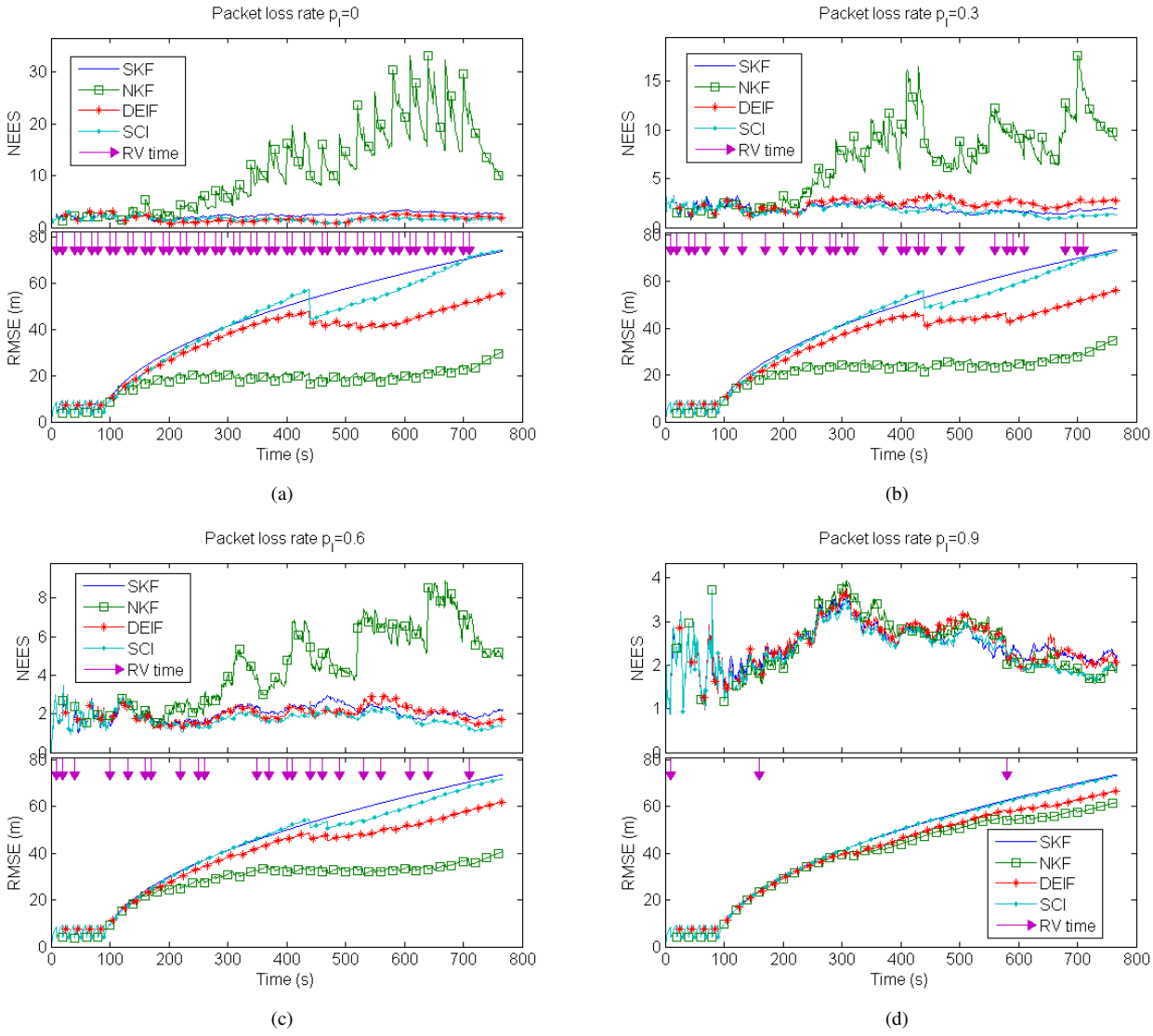

Fig. 5. Simulation results for Vehicle 3 at packet loss rate (a) $p_l = 0$ (b) $p_l = 0.3$ (c) $p_l = 0.6$ and (d) $p_l = 0.9$. The vertical arrows show the times when Vehicle 3 receives broadcast.

We can see that with more frequent cooperation, SCI tends to be over conservative about its estimation and even gives poorer estimated error covariance than SKF. In the other hand, DEIF estimation maintains good consistency and performs better than SCI across all occasions.

B. Experimental data

Navigation data from an experiment is used in the offline processing to compare different estimation filters. In the experiment, GPS logs are used as the benchmark to compute positioning errors. The arrows in Fig. 6 indicate the times when the broadcasts are sent and successfully received by other vehicles. In the first 100 seconds, Vehicles 1 and 3 have good local measurements. Vehicle 2 exhibits a slow position drift with the information shared by Vehicles 1 and 3. Vehicle 2 obtains good local measurements from 200 to 300 seconds, and from 600 seconds onwards. The proposed DEIF successfully improves estimation accuracy of all vehicles. In the two highlighted boxes, we can see that Vehicles 1 and 3 get position improvements from the broadcast given by Vehicle 2. Meanwhile, Vehicle 2 also benefits from the information sharing (at 400 seconds). On the other hand, the localization improvement for Vehicle 1 is lower when using an NKF. For Vehicles 2 and 3, the localization by NKF is even worse than the single vehicle localization (SKF).

VI. Conclusion and Future Work

We described the design and implementation of a distributed extended information filter for cooperative multi-AUV localization. This DEIF is especially suitable for underwater vehicles where the communication links have the problems of limited bandwidth and lossy packets. The effectiveness and

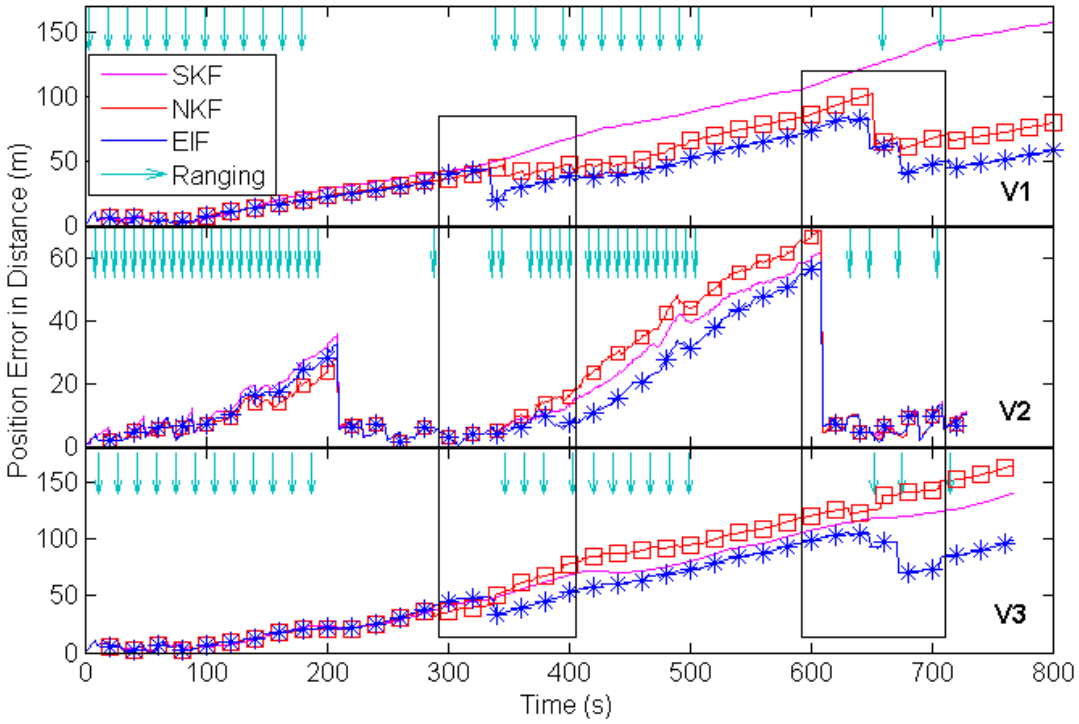

Fig. 6. Cooperative localization results with field data.

advantages have been demonstrated by illustrative examples, and comparative results from simulated and experimental data.

In fact, multi-vehicle cooperative localization is one type of data fusion in cooperative intelligent vehicles. Data fusion, which aims at integration of data and knowledge from multiple sources, is an important process to achieve better state estimation. In a multi-AUV mission, the proposed method can also be used for applications such as cooperative object tracking, cooperative environment sensing and map building.

REFERENCES

[1] Y. T. Tan, M. Chitre, and F. S. Hover, "Cooperative bathymetry-based localization using low-cost autonomous underwater vehicles," *Autonomous Robots*, pp. 1–19, 2015.

[2] A. Bahr, *Cooperative Localization for Autonomous Underwater Vehicles*. PhD thesis, the Massachusetts Institute of Technology and the Woods Hole Oceanographic Institution, February 2009.

[3] J. K. Uhlmann, "Covariance consistency methods for fault-tolerant distributed data fusion," *Information Fusion*, vol. 4, pp. 201–215, September 2003.

[4] A. Benaskeur, "Consistent fusion of correlated data sources," in *IECON 02 [Industrial Electronics Society, IEEE 2002 28th Annual Conference of the]*, vol. 4, pp. 2652–2656 vol.4, 2002.

[5] Y. Zhou and J. Li, "Data fusion of unknown correlations using internal ellipsodal approximation," in *Proceedings of the 17th World Congress, The International Federation of AUtomatic Control Seoul, Korea*, July 2008.

[6] H. Li, F. Nashashibi, and M. Yang, "Split covariance intersection filter: Theory and its application to vehicle localization," *Intelligent Transportation Systems, IEEE Transactions on*, vol. 14, no. 4, pp. 1860–1871, 2013.

[7] R. M. Eustice, H. Singh, and J. J. Leonard, "Exactly sparse delayed-state filters for view-based slam," *IEEE Transactions on Robotics*, vol. 22, pp. 1100–1114, Dec 2006.

[8] S. E. Webster, J. M. Walls, L. L. Whitcomb, and R. M. Eustice, "Decentralized extended information filter for single-beacon cooperative acoustic navigation: Theory and experiments," *IEEE Transactions on Robotics*, vol. 29, pp. 957–974, Aug 2013.

[9] R. Kalman, "A new approach to linear filtering and prediction problems," *Journal of Basic Engineering*, 1960.

[10] B. Kalyan and M. Chitre, "A feasibility analysis on using bathymetry for navigation of autonomous underwater vehicles," in *Proceedings of the 28th Annual ACM Symposium on Applied Computing*, SAC '13, (New York, NY, USA), pp. 229–231, ACM, 2013.

[11] Y. Bar-Shalom, *Multitarget-Multisensor Tracking: Principles And Techiniques*. YBS Publishing, 3rd ed., 1995.

[12] H. Li and F. Nashashibi, "Cooperative multi-vehicle localization using split covariance intersection filter," *Intelligent Transportation Systems Magazine, IEEE*, vol. 5, pp. 33–44, Summer 2013.